ISSN 0026-8933, Molecular Biology, 2006, Vol. 40, No. 2, pp. 276–283. © Pleiades Publishing, Inc., 2006.
Original Russian Text © S.L. Grokhovsky, 2006, published in Molekulyarnaya Biologiya, 2006, Vol. 40, No. 2, pp. 317–325.

STRUCTURAL–FUNCTIONAL ANALYSIS OF BIOPOLYMERS AND THEIR COMPLEXES

UDC 577.323.5;577.31;577.356;577.113.7

Specificity of DNA Cleavage by Ultrasound

S. L. Grokhovsky

Engelhardt Institute of Molecular Biology, Russian Academy of Sciences, Moscow, 119991 Russia; e-mail: grok@imb.ac.ru

Center of Medical Research, University of Oslo, Moscow, 119991 Russia

Received July 1, 2005

Abstract—Cleavage of double-stranded DNA fragments with known nucleotide sequences upon sonication at 22 and 44 kHz was studied by PAGE. The cleavage rate was shown to depend on the fragment size, pH, ionic strength, and temperature. Double-strand breaks occurred preferentially in 5'-CpG-3' dinucleotides. The strand was broken between C and G so that the phosphate group was at the 5' side of G in the products. The cleavage rate proved to depend on the sequences flanking the cleavage site. The character of cleavage changed in the presence of Pt-bis-netropsin, a sequence-specific ligand that alters the local conformation of DNA.

DOI: 10.1134/S0026893306020142

Key words: ultrasound, DNA cleavage, 5'-CpG, DNA conformation, sequence-specific ligands

INTRODUCTION

Genomic DNA occurs as a single circular molecule in the prokaryotic cell and as several linear molecules per each chromosome in the eukaryotic cell. Such DNA molecules vary in length from a fraction of a millimeter in prokaryotes to several centimeters in eukaryotes. To illustrate, if the diameter of a molecule were increased to 2 cm, its length would be several hundreds of kilometers. In the cell, DNA is folded and condensed owing to complexes of histones in eukaryotes and histone-like proteins in prokaryotes. The combination of a macroscopic length with a microscopic diameter makes it possible to study the properties of double-stranded DNA upon exposure to various physical factors. DNA cleavage with ultrasound was widely employed in early studies of DNA [1, 2]. High-intensity sonication of double-stranded DNA in an aqueous solution causes mostly double-strand breaks and yields fragments of several hundreds of base pairs [3, 4]. Yet there is no information in the available literature concerning comparison of the extent of cleavage for different sequences or the character of the terminal nucleotides in the resulting DNA fragments. The objective of this work was to study the specificity of breaks arising in the sugar–phosphate backbone upon sonication of DNA fragments with known sequences.

DNA breaks caused by acoustic waves have been explained by cavitation, that is, generation of cavities filled with vapor (cavitation bubbles) when an acoustic wave passes through a solution [5, 6]. At the moment of collapse, high temperatures and pressures develop inside cavitation bubbles and even high-voltage discharges are possible because a double electrical layer is formed on the bubble surface. Cavitation does not occur until acoustic waves reach a certain threshold intensity. It is clear that only part of the energy is expended for generating cavitation bubbles by ultrasound waves passing through a fluid. The other part goes into generating microflows, heating the fluid, forming a fountain, and spraying the fluid. The energy of collapsing bubbles goes into the radiation of shock waves, local heating of the gas and the fluid, generation of free radicals, and some other processes [7]. There is evidence that the suppression of cavitation prevents the destruction of some polymers. It is thought that polymeric chains break mostly under the action of extremely high forces arising in rapid flows near collapsing cavitation bubbles and shock waves arising as bubbles disappear [8]. The results of this work testify again that the mechanical forces of local microflows, rather than reactive radicals, play the major role in causing DNA breaks. DNA strands break mostly at sites with an altered local conformation of the double helix.

EXPERIMENTAL

DNA fragments. To obtain DNA fragments, modified pGEM7(f+) (Promega), which contained synthetic oligonucleotides in the polylinker [9], was digested with *Nco*I and *Apa*I to yield 470- and 475-bp fragments or with *Xba*I and *Bgl*II (Promega) to yield a 439-bp fragment. In addition, pUC9 was digested with *Dde*I (Promega) to yield a 166-bp fragment. The sequences of the fragments are shown in the figures. The 166-bp fragment was 3'-endlabeled with [α-^{33}P]dCTP

and the other fragments, with [α-^{33}P]dATP (Institute of Reactor Materials, Zarechnyi, Russia) in the presence of the nonlabeled other dNTPs and the Klenow fragment of *Escherichia coli* DNA polymerase I (Boehringer-Mannheim, Germany). The DNA fragments were isolated by PAGE in 1-mm thick 5% gel with subsequent elution and precipitation [10].

Sonication of DNA fragments in solution. To obtain samples for sonication, 5 μl of a DNA fragment (approximately 10^4 Bq) in 5 mM NaOAc, pH 7.0 (unless otherwise indicated) were combined with 5 μl of the same buffer or a ligand dissolved in the same buffer in 0.2-ml thin-walled polypropylene tubes (Perkin-Elmer, United States). The final concentration of the fragment was 5–10 μg/ml (~10 μM base pair).

Samples were sonicated using an UZDN-2T ultrasound dispergator (Ukraine) at 44 or 22 kHz. Tubes were placed into a Teflon ring which had a 15-mm central hole and radial tube accommodation holes, so that the ends of the tubes were 1 cm below the surface of the radiator end. The ring was placed in a bath filled with water and finely ground ice (unless otherwise indicated) and rotated at 2 rpm.

Nondenaturing PAGE. After sonication, the sample was combined with an equal volume of 50% glycerol with 0.02% Bromphenol Blue. Aliquots (0.5 μl) were applied on PAAG of 40 cm in length and 0.15 mm in thickness. Electrophoresis was carried out in 1 × TBE at 1.3 kV (~30 W) for 3 h (gel temperature ~30°C) or at 300 V (~1 W) for 18 h at +2°C. Gels were dried on a glass which was pretreated with γ-methacrylpropyloxysilane (LKB, Sweden); they were then exposed with a Kodak X-ray film (United States) or with a luminescent screen. Sequencing was carried out using a Cyclone Storage Phosphor system (Packard BioScience, United States).

Denaturing PAGE. After sonication, the sample was combined with 90 μl of 0.15 M NaCl, 50 mM Tris-HCl (pH 7.5), 10 mM EDTA, and 10 μg/ml tRNA. The resulting mixture was extracted with phenol. DNA was precipitated with ethanol, washed with 70% ethanol, dried, and dissolved in 1 μl of 95% formamide, 15 mM EDTA (pH 8.0), 0.05% Bromphenol Blue, 0.05% xylene cyanole FF; it was subsequently heated at 90°C for 1 min, quickly chilled at 0°C, and applied on denaturing PAAG (length 40 cm, thickness gradient 0.15–0.45 mm) [11]. Electrophoresis was carried out at 100 W (2.3 kV) at 60–70°C for 55 min. Gels were fixed with 10% acetic acid, dried on a glass, and exposed as above.

RESULTS AND DISCUSSION

Cleavage as Dependent on the DNA Fragment Size, Ultrasound Frequency, pH, and Ionic Strength

Cleavage profiles of the 470-bp DNA fragment were obtained by nondenaturing PAGE (Fig. 1). The fragment contained AT clusters alternating with GC clusters. PAGE was carried out at 2°C (Fig. 1a). A similar pattern was observed when PAGE was carried out at 30°C (Fig. 1b). This temperature makes it possible to detect double-strand breaks with cleavage sites located several nucleotides apart on the two DNA strands: such sticky ends melt during PAGE under these conditions.

As Fig. 1 shows, the fragment was cleaved preferentially at several sites, which corresponded to alternating GC pairs. Many double-strand breaks arose as early as within the first four minutes of sonication. Further sonication enhanced the cleavage pattern, but the ends of the fragment still remained noncleaved. It is probable that the ends of fragments are sufficiently flexible and difficult to break. The efficiency of cleavage slightly increased with ionic strength increasing from 5 mM to 0.5 M at pH 7.0. When pH was varied, cleavage was almost undetectable at pH 11.0, while its efficiency considerably increased at pH 5.0. This finding is explained by the fact that the double helix is partly unwound at alkaline pH, which increases the flexibility and the condensation of DNA. Acidic pH expedites the proton attack on the phosphodiester bond. When sonication temperature was increased to 30°C, cleavage was almost completely suppressed (Fig. 1c). The fragment was cleaved to a significant extent at 30°C only at low pH. These findings suggest that the main contribution to breaking DNA strands is made by hydrodynamic forces which arise when cavitation bubbles collapse and which depend on the water vapor pressure, decreasing with a decrease in temperature [8]. The chemical processes generating radicals during cavitation play only a minor role, if any.

The character of fragment cleavage was the same upon sonication at 22 and at 44 kHz.

Sequence Dependence of the DNA Cleavage Rate

To localize the DNA cleavage sites, the sonication product was resolved by denaturing PAGE. Figure 2 shows the cleavage patterns of the 475- and 439-bp fragments. The fragments carried the label on different strands of the same sequence: one 3' end of each fragment was labeled. PAGE reports breaks for only one strand under such conditions. Several sites were revealed whose cleavage rate was considerably higher than the background level. Preliminary analysis of the nucleotide sequence of these and other (data not shown) fragments demonstrated that DNA strands break more readily between cytosine and guanine in

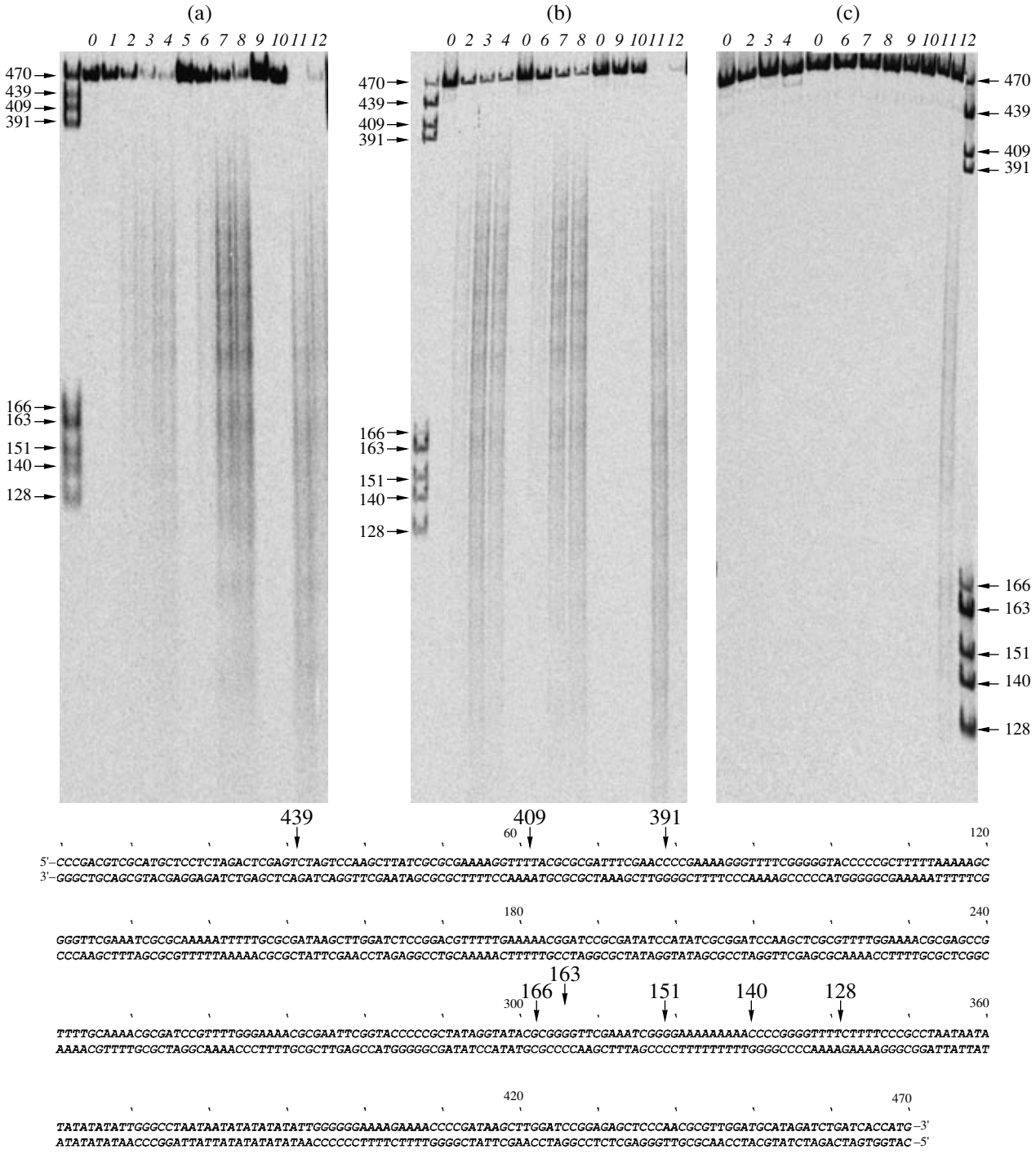

Fig. 1. Cleavage profiles of the 470-bp DNA fragment in nondenaturing 5% PAAG after sonication at 44 kHz. DNA was (a) sonicated at 0°C and resolved at 2°C, (b) sonicated at 0°C and resolved at 30°C, or (c) sonicated at 30°C and resolved at 30°C. The fragment sequence is shown at the bottom. Positions of labeled marker double-stranded DNA fragments of known sizes are shown with arrows on the electrophoretic patterns and on the sequence. The fragment was analyzed (*0*) before and after sonication (*1–4*) in 5 mM NaOAc (pH 7.0) for 2, 4, 8, and 16 min, respectively; (*5–8*) in 0.5 M NaOAc (pH 7.0) for 2, 4, 8, and 16 min, respectively; (*9*, *10*), in 0.5 M NaOAc (pH 11.0) for 4 and 8 min, respectively; and (*11*, *12*) in 0.5 M NaOAc (pH 5.0) for 4 and 8 min, respectively.

the 5'-CpG-3' sequence. The cleavage rate of this sequence depended on its nucleotide context. Cleavage was intense when the sequence was flanked by mixed sequences which contained all four nucleotides and had both purines and pyrimidines in each strand. Weaker cleavage was observed when 5'-CpG-3' was flanked by sequences having purines only in one strand. In addition, the cleavage rate was higher than

the background level when the cleavage site was at the boundary between a mixed sequence and a sequence having purines only in one strand.

Ligands Affecting the Local Conformation of the DNA Double Helix Change the DNA Cleavage Rate

The above data suggest that sonication can be used to probe the local conformation of the DNA double helix. The structure of double-stranded DNA is not perfectly monotonous, but depends on the nucleotide sequence [12–15]. The nucleotides differ in geometry, and their combinations show various deviations from the ideal helical structure: bends, turns, and changes in the widths of the minor and major grooves. Such features are of importance for DNA condensation and recognition by various proteins in the cell.

In addition, structural changes arise in DNA when the parameters of its aqueous environment are changed or various ligands are bound. A convenient model for studying the local parameters of the double helix is provided by low-molecular-weight sequence-specific ligands, which bind to particular DNA sequences [16, 17]. To localize certain ligands on DNA, advantage can be taken of the selective adsorption of X-rays by heavy metal atoms [18–20]. Pt-bis-netropsin was used in such experiments and was localized in the DNA minor groove on a fragment with a known sequence (Fig. 3) [18]. Sites where the sugar–phosphate backbone was cleaved in both strands (long arrows) were detected in regions tightly bound with Pt-bis-netropsin and corresponded to the position of the platinum atom. Netropsin residues oriented differently relative to the DNA helix recognize two symmetrical consensus sequences, 5'-TTTT-3' (underlined). A scheme of the complex of Pt-bis-netropsin with DNA is shown on the right.

However, it remained unclear why minor cleavage sites are detectable in a sequence of alternating AT pairs. More recent analysis of the binding of Pt-bis-netropsin with double-stranded oligonucleotides revealed complexes of another type [21]. In this case, two netropsin residues of a Pt-bis-netropsin molecule are arranged as a parallel pin which forms a tight complex with a sequence of four alternating AT pairs (Fig. 3, left scheme).

When a complex of Pt-bis-netropsin with this fragment was sonicated (Fig. 3, on the left), the background cleavage rate was slightly decreased in sites where the ligand was bound to DNA in the extended conformation. A local increase in cleavage was observed at nucleotides adjacent to the sites where Pt-bis-netropsin pins were bound (wavy arrows). Similar regions where the cleavage rate decreased or increased depending on the conformation of Pt-bis-netropsin in complex with DNA sequences containing thymines or alternating AT pairs in one strand are detectable in Fig. 2 (lanes *5–7*).

Character of the Terminal Groups Resulting from DNA Cleavage

Chemical cleavage of DNA with formic acid eliminates a purine from the cleavage site [22]. Thus, the bands seen in lanes A + G (Figs. 2, 3) correspond to oligonucleotides lacking the terminal purine. 3'-End-labeled fragments contain the uncharged 3'-OH group at the 3' end and the phosphate group, which carries two negative charges, at the 5' end. When the 5'-terminal phosphate is removed with phosphatase, the electrophoretic mobility of DNA fragments changes (Fig. 2; lanes *1*, *2*). The mobility of a fragment depends on its molecular weight, its total charge, and the gel density. The longer the fragment, the lower the contribution of the two terminal charges to the total charge and the stronger the dependence of the electrophoretic mobility on the fragment size. For instance, electrophoretic mobility shifts by 1.5 steps in the region of 20-mer oligonucleotides, by 1 step in the region of 40-mer oligonucleotides, and by 0.5 steps in the region of 90-mer oligonucleotides in denaturing 6% PAAG. In 14% gel, similar shifts are observed in the regions of 14-, 25-, and 55-mer oligonucleotides, respectively.

The bands observed after sonication of the DNA fragment coincided with the bands observed after its chemical cleavage at purines (Figs. 2, 3). This result indicated that the products had phosphates at their 5' ends.

The above data on the effect of ultrasound on DNA fragments allow several conclusions concerning the sequence dependence of the DNA strength and the biological consequences of this dependence.

Since fragment ends of less than 30–50 bp escape cleavage almost completely, the cavitaion hydrodynamic impacts arising upon sonication affect extended DNA regions of about 100 bp. Short DNA fragments of less than 50 bp are virtually noncleavable by sonication. A similar effect has been described for various polymers [8]. When a minor amount of more labile bonds is introduced in a polymeric chain, its degradation by ultrasound increases dramatically [23]. These findings make it possible to assume that DNA cleavage sites reflect the dependence of the strength of phosphodiester bonds in the sugar–phosphate backbone on the local conformation of nucleotide combinations. Under normal conditions, cell DNA is exposed to similar loads during chromosome segregation, replication, transcription, and some other processes. Hence, this characteristic is probably reflected in the DNA sequences of various organisms.

As the above results demonstrate, DNA is most readily cleaved at the 5'-CpG-3' dinucleotide upon sonication. This dinucleotide occurs at an appreciably

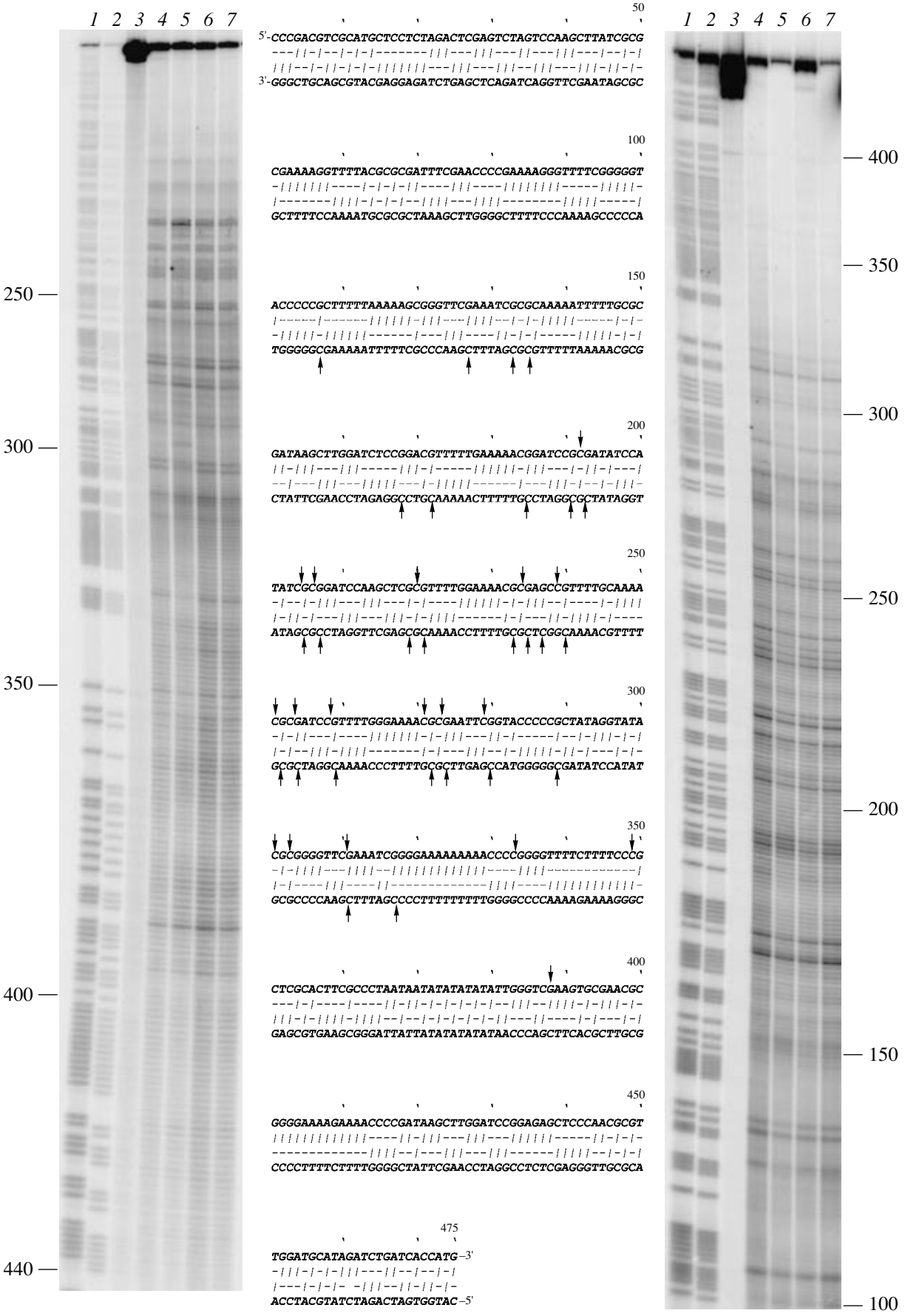
1 2 3 4 5 6 7
250
300
350
400
440
5'-CCCGACGTCGCATGCTCCTCTAGACTCGAGTCTAGTCCAAGCTTATCGCG
3'-GGGCTGCAGCGTACGAGGAGATCTGAGCTCAGATCAGGTTCGAATAGCGC
CGAAAAGGTTTTACGCGCGATTTCGAACCCCGAAAAGGGTTTTCGGGGGT
GCTTTTCCAAAATGCGCGCTAAAGCTTGGGGCTTTTCCCAAAAGCCCCCA
ACCCCCGCTTTTTAAAAAGCGGGTTCGAAATCGCGCAAAAATTTTTGCGC
TGGGGGCGAAAAATTTTTCGCCCAAGCTTTAGCGCGTTTTAAAAACGCG
GATAAGCTTGGATCTCCGGACGTTTTTGAAAAACGGATCCGCGATATCCA
CTATTCGAACCTAGAGGCCTGCAAAAACTTTTTGCCTAGGCGCTATAGGT
TATCGCGGATCCAAGCTCGCGTTTTGGAAAACGCGAGCCGTTTTGCAAAA
ATAGCGCCTAGGTTCGAGCGCAAAACCTTTTGCGCTCGGCAAAACGTTTT
CGCGATCCGTTTTGGGAAAACGCGAATTCGGTACCCCCGCTATAGGTATA
GCGCTAGGCAAAACCCTTTTGCGCTTGAGCCATGGGGGCGATATCCATAT
CGCGGGGTTCGAAATCGGGGAAAAAAAAACCCCGGGGGTTTTCTTTTCCCG
GCGCCCCAAGCTTTAGCCCCTTTTTTTTTGGGGCCCCAAAAGAAAAGGGC
CTCGCACTTCGCCCTAATAATATATATATATTGGGTCGAAGTGCGAACGC
GAGCGTGAAGCGGGATTATTATATATATATAACCCAGCTTCACGCTTGCG
GGGGAAAAGAAAACCCCGATAAGCTTGGATCCGGAGAGCTCCCAACGCGT
CCCCTTTTCTTTTGGGGCTATTCGAACCTAGGCCTCTCGAGGGTTGCGCA
TGGATGCATAGATCTGATCACCATG–3'
ACCTACGTATCTAGACTAGTGGTAC–5'
50
100
150
200
250
300
350
400
450
475
1 2 3 4 5 6 7
400
350
300
250
200
150
100

Fig. 2. Cleavage profiles of the 475- and 439-bp DNA fragments in denaturing 6% PAAG after sonication at 44 kHz for 20 min. Lane *1*, products of chemical cleavage at purines with subsequent treatment with phosphatase; *2*, product of chemical cleavage at purines; *3*, the initial fragment without treatment; *4*, the fragment sonicated in isolation; and *5–7*, the fragment sonicated in the presence of 1, 0.5, or 0.25 μM of Pt-bis-netropsin, respectively. The cleavage profiles are shown on the left for the 475-bp fragment (the upper strand is radiolabeled) and on the right for the 439-bp fragment (the lower strand is radiolabeled). The nucleotide sequence of the fragments is shown in the center. To simplify comparison with the bands seen on gels, purines are marked with slants for each strand. The sites with a cleavage rate far higher than the background level are indicated with arrows.

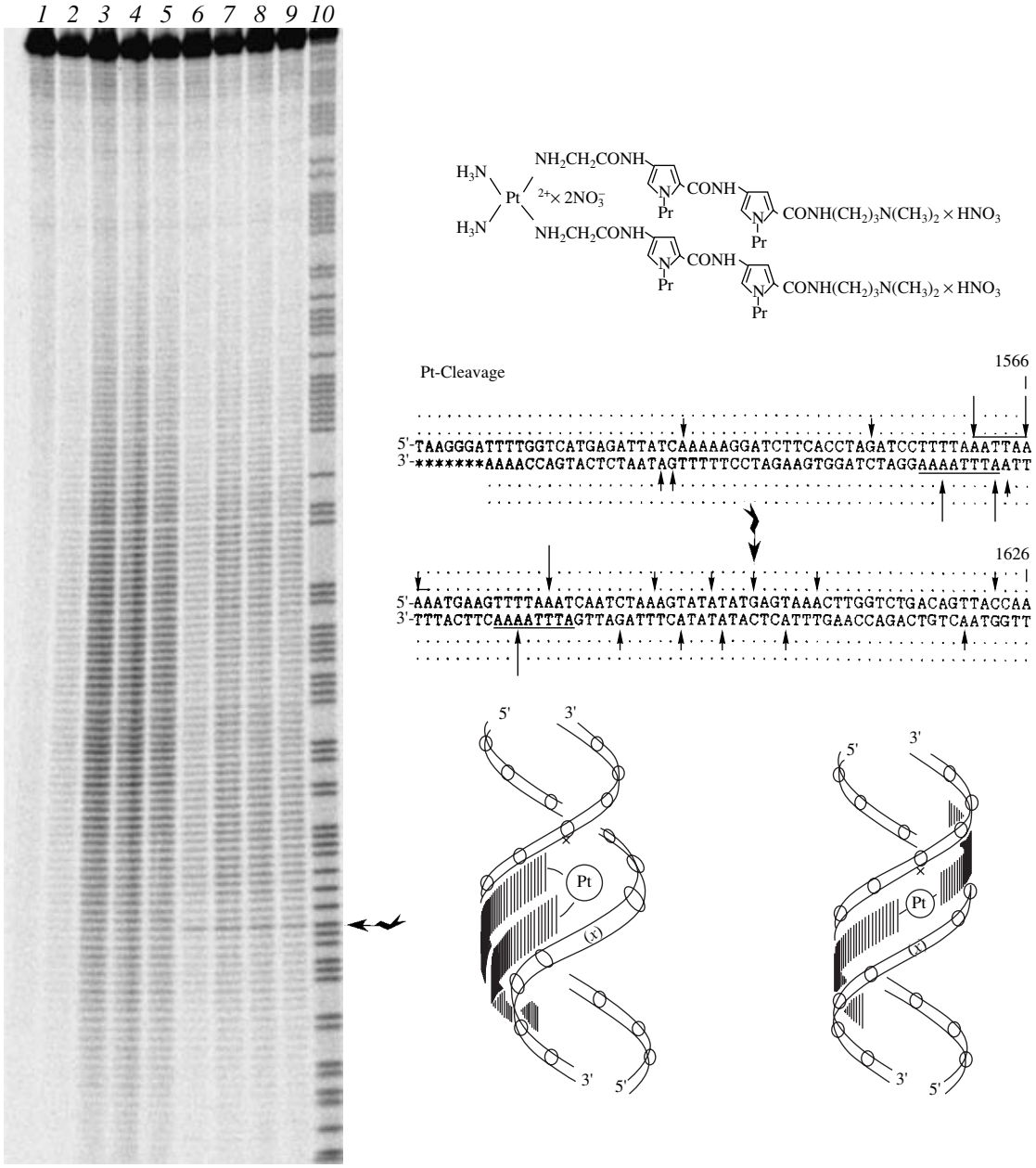

Fig. 3. Cleavage profile of the 166-bp fragment in denaturing 6% PAAG after sonication at 44 kHz. The fragment was analyzed (*1*) before and (*2–5*) after sonication for 2, 4, 8, and 16 min, respectively; (*6–9*) sonication in the presence of 0.5 μM Pt-bis-netropsin for 2, 4, 8, and 16 min, respectively; and (*10*) chemical cleavage at purines. Plain arrows indicate the sites of complex cleavage upon exposure to X-rays [18]. A wavy arrow indicates the site where sonication-induced cleavage became more intense.

reduced frequency in the genomes of many organisms, with a few noteworthy exceptions such as *Heamophilus influenzae* and *Niesseria gonorrhoeae*, which are highly competent, that is, capable of integrating foreign DNA into their genomes [24]. The low frequency of the 5'-CpG-3' dinucleotide in vertebrate DNA is usually explained by the classical scenario methylation–deamination–mutation, which leads to the substitution of 5'-TpG-3'/5'-CpA-3' for 5-CpG-3' [25, 26]. Yet this hypothesis fails to explain the low frequency of 5'-CpG-3' in animal mitochondrial DNA and in the genomes of some organisms lacking CpG-methylase activity. The normal presence of 5'-CpG-3' in the genomes of insects, worms, and most fungi probably reflects the specifics of their replication systems or the more compact packing of nucleosomes in chromatin. It is possible to assume that the presence of islands with a high content of 5'-CpG-3' upstream and downstream of structural genes provides a mechanism of gene shuffling during evolution. Epigenetic mechanisms based on 5'-CpG-3' methylation may be secondary, arising because the enzyme recognizes the unusual structure of the 5'-CpG-3' dinucleotide or flips cytosines out of the DNA helix during methylation more efficiently then the other bases.

Comparison of the results with published data yielded a paradox: according to quantum mechanical computations, the 5'-CpG-3' dinucleotide (and 5'-GpC-3' as well) contained in B-DNA has the lowest free energy as compared with the other dinucleotides. The stacking conditions are optimal for the two pairs of the dinucleotide, suggesting a greater stability of the bond between them [27, 28]. On the other hand, the mechanical properties of single DNA molecules [29] better agree with the idea that DNA is a vermiform chain [30, 31], which is flexible and even capable of knotting [32]. According to this model, specific breaks caused by the difference in stacking between adjacent base pairs are unlikely. The discrepancy between the experimental findings and modeling data can be explained by the fact that quantum mechanical computations yield a picture at the molecular level and take into account neither the macromolecular characteristics of DNA, such as local transitions from the B to the Z conformation [33, 34], nor the cluster properties of water [7]. Experiments with single DNA molecules consider periods of tens of seconds, which are sufficient for the complete relaxation of transition states. It is possible to assume that the time it takes for cavitation hydroacoustic impacts to affect DNA better corresponds to the actual periods of cell processes proceeding at the boundary of the molecular and macromolecular levels.

ACKNOWLEDGEMENTS

I am grateful to O.V. Preobrazhenskaya and V.I. Popenko for help in experiments and discussion of the results.

This study was supported by the Russian Foundation for Basic Research (project nos. 04-04-49364, 04-03-33144, 03-04-48903) and the program Molecular and Cell Biology of the Russian Academy of Sciences.

REFERENCES

1. Doty P., McGill B.B., Rice S.A. 1958. The properties of sonic fragments of deoxyribosenucleic acid. *Proc. Natl. Acad. Sci. USA*. **44**, 432–438.
2. Davison P.F., Freifelder D. 1962. Studies on the sonic degradation of deoxyribonucleic acid. *Biophys. J*. **2**, 235–247.
3. Randolph M.L., Setlow J.K. 1972. Mechanism of inactivation of *Haemophilus influenzae* transforming deoxyribonucleic acid by sonic radiation. *J. Bacteriol*. **111**, 186–191.
4. Mann T.L., Krull U.J. 2004. The application of ultrasound as a rapid method to provide DNA fragments suitable for detection by DNA biosensors. *Biosens. Bioelectronics*. **20**, 945–955.
5. Miller D.L., Thomas R.M. 1996. The role of cavitation in the induction of cellular DNA damage by ultrasound and lithotripter shock waves in vitro. *Ultrasound Med. Biol*. **22**, 681–687.
6. Fuciarelli A.F., Sisk E.C., Thomas R.M., Miller D.L. 1995. Induction of base damage in DNA solutions by ultrasonic cavitation. *Free Rad. Biol. Med*. **18**, 231–238.
7. Margulis M.A. 1984. *Osnovy zvukokhimii* (Fundamentals of Acoustic Chemistry). Moscow: Khimiya.
8. Suslick K.S., Price G.J. 1999. Applications of ultrasound to materials chemistry. *Annu. Rev. Mater. Sci*. **29**, 295–326.
9. Grokhovsky S.L., Surovaya A.N., Burckhardt G., Pismensky V.F., Chernov B.K., Zimmer Ch., Gursky G.V. 1998. DNA sequence recognition by bis-linked netropsin and distamycin derivatives. *FEBS Lett*. **439**, 346–350.
10. Maniatis, T., Fritsch, E.F., Sambrook, J. 1982. *Molecular Cloning: A Laboratory Manual*. Cold Spring Harbor, N.Y.: Cold Spring Harbor Lab. Press.
11. Kraev A.S. 1988. A simple system for phage M13 cloning and DNA sequencing with the use of terminators. *Mol. Biol*. **22**, 1164–1197.
12. Dickerson R.E., Drew H.R. 1981. Structure of a B-DNA dodecamer: 2. Influence of base sequence on helix structure. *J. Mol. Biol*. **149**, 761–786.
13. Hyeon-Sook K., Crothers D.M. 1988. Calibration of DNA curvature and a unified description of sequence-directed bending. *Proc. Natl. Acad. Sci. USA*. **85**, 1763–1767.
14. Sarai A., Mazur J., Nussinov R., Jernigan R.L. 1988. Origin of DNA helical structure and its sequence dependance. *Biochemistry*. **27**, 8498–8502.

15. Chuprina V.P., Heinemann U., Nurislamov A.A., Zielenkiewicz P., Dickerson R.E., Saender W. 1991. Molecular dynamics simulation of the hydration shell of a B-DNA decamer reveals two main types of minor-groove hydration depending on groove width. *Proc. Natl. Acad. Sci. USA*. **88**, 593–597.

16. Zasedatelev A.S., Zhuze A.L., Zimmer K., Grokhovsky S.L., Tumanyan V.G., Gursky G.V., Gottikh B.P. 1976. A stereochemical model of the molecular mechanism of AT pair recognition upon distamycin A and netropsin binding to DNA. *Dokl. Akad. Nauk SSSR*. **231**, 1006–1009.

17. Gursky G.V., Zasedatelev A.S., Zhuze A.L., Khorlin A.A., Grokhovsky S.L., Streltsov S.A., Surovaya A.N., Nikitin S.M., Krylov A.S., Retchinsky V.O., Mikhailov M.V., Beabealashvili R.S., Gottich B.P. 1983. Synthetic sequence-specific ligands. *Cold Spring Harbor Symp. Quant. Biol*. **47**, 367–378.

18. Grokhovsky S.L., Zubarev V.E. 1991. Sequence-specific cleavage of double-stranded DNA caused by X-ray ionization of the platinum atom in the Pt-bis-netropsin–DNA complex. *Nucleic Acids Res*. **19**, 257–264.

19. Grokhovsky S.L., Gottikh B.P., Zhuze A.L. 1992. Ligands with affinity for certain DNA sequences: 9. Sythesis of netropsin and distamycin A analogs containing a sarcolysin residue or a platinum (II) atom. *Bioorg. Khim*. **18**, 570–583.

20. Grokhovsky S.L., Nikolaev V.A., Zubarev V.E., Surovaya A.N., Zhuze A.L., Chernov B.L., Sidorova N.Yu., Zasedatelev A.S., Gursky G.V. 1992. Specific DNA cleavage by a netropsin analog containing the copper ion (II)-chelating Gly-Gly-His peptide. *Mol. Biol*. **26**, 1274–1297.

21. Surovaya A.N., Grokhovsky S.L., Burkhardt H., Fritsche H., Zimmer K., Gursky G.V. 2002. Effect of local DNA conformation in bis-netropsin binding to DNA. *Mol. Biol*. **36**, 901–911.

22. Belikov S., Wieslander L. 1995. Express protocol for generating G + A sequencing ladders. *Nuclei Acids Res*. **23**, 310.

23. Encina M.V., Lissi E., Sarasua M., Gargallo L., Radic D. 1980. Ultrasonic degradation of polyvinylpyrrolidone: Effect of peroxide linkages. *J. Polym. Sci. Polym. Letter*. **18**, 757–760.

24. Karlin S., Campbell A.M., Mrazek J. 1998. Comparative DNA analysis across diverse genomes. *Annu. Rev. Genet*. **32**, 185–225.

25. Doerfler W. 1983. DNA methylation and gene activity. *Annu. Rev. Biochem*. **52**, 93–124.

26. Tazi J., Bird A. 1990. Alternative chromatin structure at CpG islands. *Cell*. **60**, 909–920.

27. SantaLucia J., Jr. 1998. A unified view of polymer, dumbbell, and oligonucleotide DNA nearest-neighbor thermodynamics. *Proc. Natl. Acad. Sci. USA*. **95**, 1460–1465.

28. Davey C.S., Pennings S., Reilly C., Meehan R.R., Allan J. 2004. A determining influence for CpG dinucleotides on nucleosome positioning in vitro. *Nucleic Acids Res*. **32**, 4322–4331.

29. Bustamante C., Smith S.B., Liphardt J., Smith D. 2000. Single-molecule studies of DNA mechanics. *Curr. Opin. Struct. Biol*. **10**, 279–285.

30. Hagerman P.J. 1988. Flexibility of DNA. *Annu. Rev. Biophys. Chem*. **17**, 265–286.

31. Cloutier T.E., Widom J. 2004. Spontaneous sharp bending of double-stranded DNA. *Mol. Cell*. **14**, 355–362.

32. Arai Y., Yasuda R., Akashi K., Harada Y., Miyata H., Kinosita K., Jr. 1999. Tying a molecular knot with optical tweezers. *Nature*. **399**, 446–448.

33. Wells R.D., Dere R.L., Hebert M., Napierala M., Son L.S. 2005. Advances in mechanisms of genetic instability related to hereditary neurological diseases. *Nucleic Acids Res*. **33**, 3785–3798.

34. Rich A., Zhang S. 2003. Z-DNA: The long road to biological function. *Nat. Rev. Genet*. **4**, 566–572.